Recent Heavy Ion Results with the ATLAS Detector at the LHC

P. Steinberg
Department of Physics, Brookhaven National Laboratory, Upton, NY, USA

Results are presented from the ATLAS collaboration from the 2010 LHC heavy ion run, during which nearly 10 inverse microbarns of luminosity were delivered. Soft physics results include charged particle multiplicities and collective flow. The charged particle multiplicity, which tracks initial state entropy production, increases by more than a factor of two relative to the top RHIC energy, with a centrality dependence very similar to that previously measured at RHIC. Measurements of elliptic flow out to large transverse momentum also show similar results to what was measured at RHIC. Extensions of these measurements to higher harmonics have also been made, and can be used to explain structures in the two-particle correlation functions that had long been attributed to jet-medium interactions. New hard probe measurements include single muons, jets and high p_T hadrons. Single muons at high momentum are used to extract the yield of $W^{\pm}$ bosons and are found to be consistent within statistical uncertainties with binary collision scaling. Conversely, jets are found to be suppressed in central events by a factor of two relative to peripheral events, with no significant dependence on the jet energy. Fragmentation functions are also found to be the same in central and peripheral events. Updated asymmetry results confirm previous measurements with increased statistics, and multiple jet cone sizes are presented. Finally, charged hadron spectra have been measured out to 30 GeV, and their centrality dependence relative to peripheral events is similar to that found for jets.

I. HEAVY IONS WITH THE ATLAS DETECTOR

The ATLAS detector at the LHC [1], shown in Fig. 1, was designed primarily for precise measurements in the highest-energy proton-proton collisions, particularly to discover new high-mass particle states. However, it is also a very capable detector for the measurement of heavy ion collisions at the highest energies achieved to date, already a factor of 14 higher than available at the Relativistic Heavy Ion Collider. The ATLAS inner detector is immersed in a 2 Tesla solenoid magnetic field and provides precise reconstruction of particle trajectories typically with three pixel layers and four double sided silicon strip detectors out to $|\eta| = 2.5$, as well as a transition radiation tracker, out to $|\eta| = 2$. The longitudinally segmented ATLAS calorimeter provides electromagnetic and hadronic measurements out to $|\eta| = 4.9$, with particularly high spatial precision in the η direction. Finally, the ATLAS Muon Spectrometer is located outside the calorimeters (which range out most of the hadronic backgrounds) and measures muon tracks out to $|\eta| < 2.7$.

The LHC provided lead-lead collisions to the three large experiments in November and December 2010, and ATLAS accumulated almost ten inverse microbarns of luminosity, as shown in the right panel of Fig. 1. The analyses shown here typically use up to eight inverse microbarns, during which the main solenoid was activated. A smaller dataset with field off was used for multiplicity analyses.

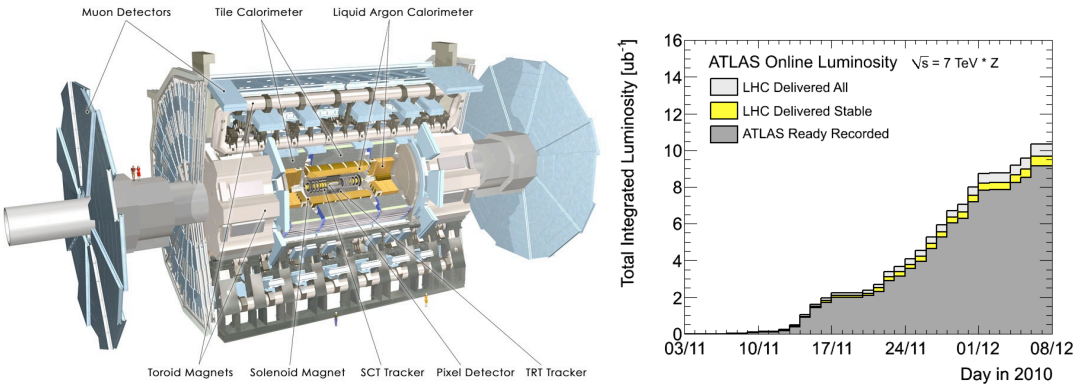

FIG. 1: (left) Schematic diagram of the ATLAS detector, showing the three main subsystems: the inner detector ($|\eta| < 2.5$), the calorimeter ($|\eta| < 4.9$) and the muon spectrometer ($|\eta| < 2.7$). (right) Integrated luminosity taken by ATLAS in the 2010 heavy ion run vs. time.

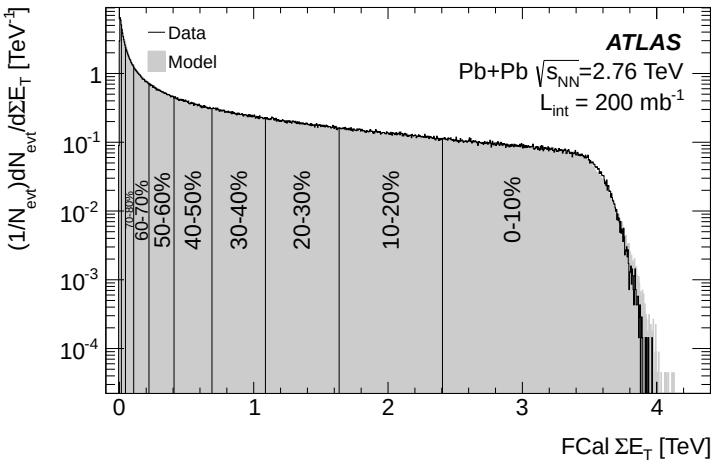

FIG. 2: Measured distribution of FCal $\Sigma E_{\rm T}$ with percentile bins indicated.

II. GLOBAL OBSERVABLES

Global observables, such as the total multiplicity and elliptic flow, address crucial issues related to the basic properties of the hot, dense medium. The charged particle multiplicity is important both from a thermodynamic standpoint, as it is proportional to the initial state entropy, as well as from the perspective of energy loss calculations which require an estimate of the initial gluon density. In ATLAS, the multiplicity has been measured [2] with the solenoid field turned off to mitigate the losses from the bending of low momentum particles. The pixel layers within $|\eta| < 2$ are used to minimize the non-primary backgrounds by only using hits consistent with a minimum-ionizing particle emanating from the primary vertex. The pixel hits are assembled both into "tracklets" (two hits, both consistent with the measured primary vertex) and full tracks (three points, reconstructed with the main ATLAS tracking software). In all, three methods are used, each with quite different systematic uncertainties, providing accurate measurements up to the highest particle densities and uncertainties of only a few percent. The collision centrality is estimated using the total transverse energy measured in the ATLAS forward calorimeter (FCal, covering $3.2 < |\eta| < 4.9$) and bins are selected using an estimated sampling fraction of $f = 100 \pm 2\%$ in the preliminary results shown at Quark Matter 2011, and a revised final value of $f = 98 \pm 2\%$ in recently-submitted papers [2, 3]. The final centrality selections [3] are shown in Fig. 2.

The final multiplicity results are shown in Fig. 3. The charged-particle yield, averaged over $|\eta| < 0.5$, $dN_{\rm ch}/d\eta/\langle N_{part}/2\rangle$ for the 6% most central events, agrees well (consistent well within the stated systematic uncertainties) with the previously-available ALICE and CMS data [4]. There is also good agreement for all centrality intervals (parametrized by N_{part}), even for the most peripheral events (as shown in detail in the inset). After scaling the RHIC data by the observed factor of 2.15, the centrality dependence at the LHC is also seen to be quite similar to that observed at a much lower energy. A similar observation was made at RHIC, by comparing data from $\sqrt{s_{NN}} = 200$ GeV to that from 19.6 GeV and finding a similar centrality dependence there as well. Given the dramatic increase in the rates of hard processes at higher energies, this seems to suggest that the centrality dependence of the charged particle density is primarily geometric in its origin.

The collective response of the system to the initial geometric configuration of the nucleons in the colliding nuclei is typically characterized by the "elliptic flow", or a $\cos(2[\phi - \Psi_2])$ modulation in the azimuthal angular distributions relative to the measured "event plane" angle Ψ_2. In ATLAS, the event plane is measured in the FCal. Elliptic flow is measured using tracks in the inner detector out to $|\eta| = 2.5$. The effects of "non flow" are minimized by maximizing the gap between the track and the event plane measurement by using the event plane from the opposite FCal hemisphere to the measured track [3]. The half-amplitude of the elliptic flow harmonic (v_2), as a function of transverse momentum and pseudorapidity, has been measured out to $p_{\rm T} = 20$ GeV and $|\eta| < 2.5$ for eight centrality bins. There is no substantial pseudorapidity dependence out to the maximum measured η, but there is a strong $p_{\rm T}$ dependence with a pronounced rise in v_2 out to $p_{\rm T} = 3$ GeV, a slower decrease out to $p_{\rm T} = 8$ GeV and then a very weak dependence out to the highest measured $p_{\rm T}$. The top panels of Fig. 4 shows the final ATLAS data on v_2 vs. $p_{\rm T}$ in eight centrality bins. The bottom panel shows the ATLAS data from the 40-50% interval compared with already-published ALICE [5] data as well as lower energy data

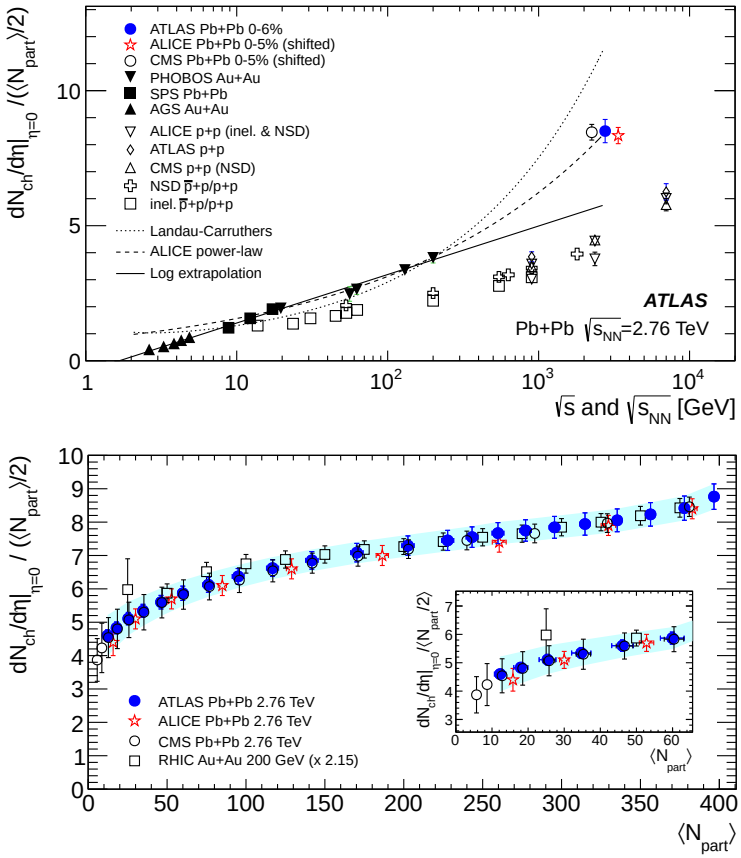

FIG. 3: (top) Energy dependence of the charged-particle multiplicity density averaged over $|\eta| < 0.5$ for the 0-6% most central events compared with heavy ion and proton-(anti)proton data [2]. (bottom) The final centrality dependence of the multiplicity per participant pair [2], compared with ALICE and CMS data and an average of the RHIC data.

from PHENIX [6] and STAR [7], all from the 40-50% centrality bin (except STAR data from 40-60%). One finds that all of the data are quite similar, even at high $p_{\rm T}$ within the large statistical errors of the PHENIX π^0 data.

It is not obvious if this apparent scaling behavior, especially at high $p_{\rm T}$, is consistent with expectations from jet energy loss. A first look at v_2 at high $p_{\rm T}$ from energy loss calculations has been made by by Horowitz and Gyulassy [8] and is shown in Fig. 5. These calculations are found to describe high $p_{\rm T}$ hadron suppression data at RHIC quite well. An extrapolation to LHC energies is performed by scaling the initial gluon density by the ratios of the charged-particle multiplicity near $\eta = 0$. However, it is found that the hadron suppression thus predicted at the LHC is a factor of two smaller than is observed in the recent LHC data (i.e. the measured R_{AA} is a factor of two higher than predicted). The predicted values of v_2 reflect the differential between energy loss of jets emitted "in plane" (i.e. which travel a shorter path length through the medium, and thus are less suppressed) and "out of plane" (which are conversely more suppressed). When compared to the preliminary ATLAS data, it is found that the data agree surprisingly well with the predictions for $p_{\rm T} > 10$ GeV and centrality above 30%. The more central data (10-20%) show a sigificant divergence from the predictions. However, this may be explained in part [9] by the lack of fluctuations in the initial nucleon configurations used in the calculations [10].

After the realization that initial state fluctuations can induce higher Fourier modes in the overlap region of the two nuclei [11], elliptic flow has now been joined by the study of higher-order harmonic flow coefficients [12]. These are measured each in their own event plane. The resolution has been evaluated by a variety of subdetector combinations and it is found that ATLAS can resolve modes up to $n = 6$ in the most central 40% of events. These are shown as a function of $p_{\rm T}$ for six centrality bins in the left panel of Fig. 6. These figures show the rapid change of v_2 with centrality, expected from previous measurements and attributed to the changing overlap geometry as the impact parameter is increased. They also show only a modest change in the higher order coefficients as the centrality changes, suggesting that they are mainly sensitive to fluctuations of nucleon positions relative to

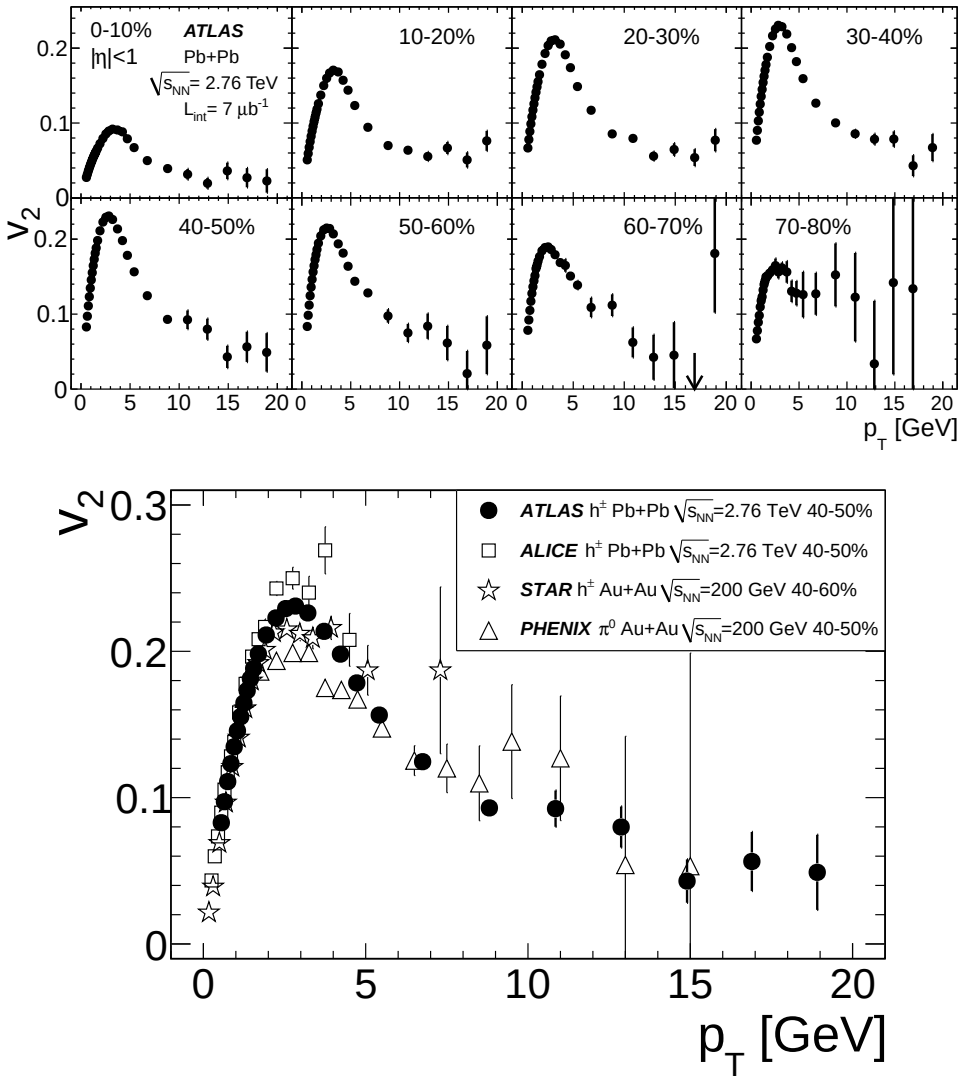

FIG. 4: (top) Elliptic flow as a function of transverse momentum integrated over $|\eta| < 1$ for eight centrality intervals (bottom) Elliptic flow as a function of transverse momentum for the 40-50% centrality interval ([3] and references therein), compared with data from RHIC and the LHC.

the overall elliptical shape given by v_2. Hydrodynamic calculations suggest a strong dependence of v_n on n, particularly when viscous effects are taken into consideration. Thus, it is expected that the information from these higher coefficients can distinguish between competing physics scenarios attempting to explain the initial state and will provide new information on the viscosity to entropy ratio.

A longstanding puzzle at RHIC is the observation of unusual structures (e.g. the Mach Cone [13]) in the two particle correlation function, particularly on the "away side" relative to a high p_{T} particle. Both STAR [14] and PHENIX [15] observed a strongly-modified away-side peak which even developed a "dip" at $\Delta\phi = \pi$ in the most central events. The "near side" is also found to show an "ridge"-like enhancement at $\Delta\phi \sim 0$ at large values of $\Delta\eta$ [16]. However, both of these phenomena have been argued to arise most likely from the presence of higher flow coefficients beyond elliptic flow [11]. In ATLAS, the correlation function has been measured with large separation in η to suppress the contribution from jets and a discrete Fourier transform (DFT) is used to extract coefficients out to $n = 6$ [3]. These are found to agree quite well with the v_n extracted using event plane approaches. More interestingly, when the event plane coefficients are used to construct a comparable two particle correlation function $dN/d\phi \propto \sum_n v_n^2 \cos(n\phi)$, one finds a striking agreement with the correlations measured directly, as shown in Fig. 6. This suggests that what were formerly thought to be indications of jet-

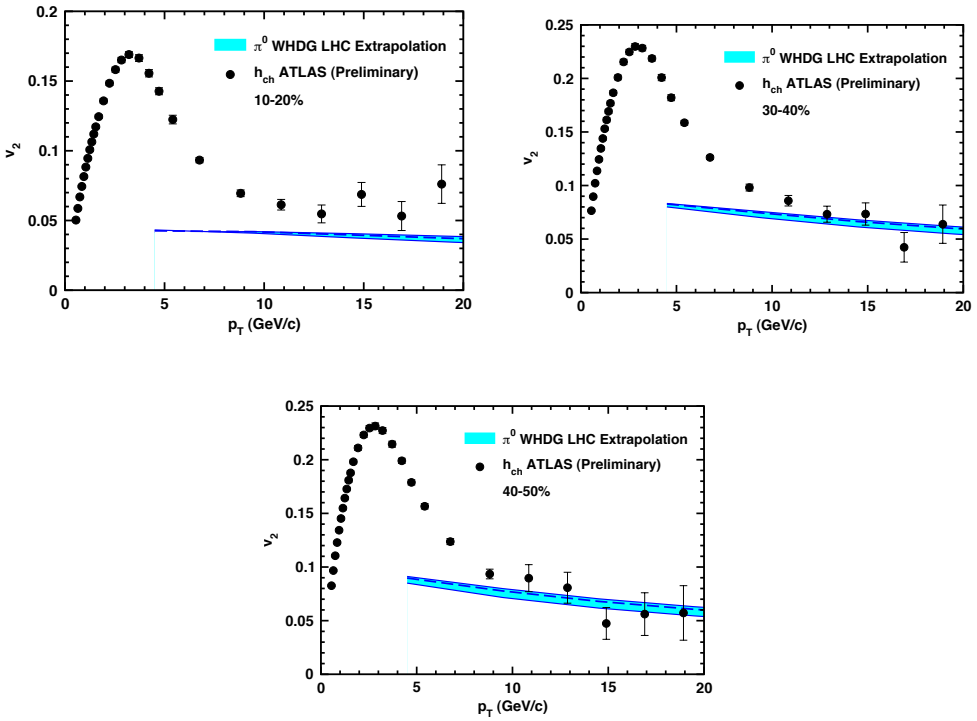

FIG. 5: Comparisons of ATLAS data of v_2 at high p_T compared with differential energy loss.

medium interactions may well result simply from the presence of higher-order flow harmonics, arising through a combination of nucleon position fluctuations and viscous effects.

III. HARD PROBES

High p_T signals produced by perturbative processes in the initial collisions of the two nuclei (also known as "hard probes") provide a means to probe the conditions of the collision at very early times. This is typically done by means of "suppression" observables which indicate deviations from the expected scaling of yields by the number of binary collisions, estimated using Glauber modeling (e.g. the ATLAS J/ψ measurement [17]). To confirm the assumed scaling, ATLAS has used the spectrum of single muons at large $p_{\rm T}$ to extract the yield of $W^{\pm}$ bosons, by a simultaneous fit of a template trained on simulated $W^{\pm}$ as well as a parameterization of muons from heavy flavor quark decays, as shown in the left panel of Fig. 7. A sample of approximately 400 W bosons has been extracted. The binary scaling of the measured yields is studied using the variable $R_{\rm PC}$, defined as the ratio of yields measured in different centrality classes to the yield measured in the 10% most central events, with all yields scaled by the corresponding number of binary nucleon-nucleon collisions. The right panel of Fig. 7 shows $R_{\rm PC}$ as a function of centrality [18]. Using a fit to a constant value, giving $\langle R_{\rm PC}\rangle = 0.99\pm0.10$ with a $\chi^2 = 3.02$ for 3 degrees of freedom, a significant consistency with binary scaling is observed.

ATLAS has already published striking results on dijet asymmetries [19]. New results are reported here on the measurement of inclusive jet yields as a function of jet $E_{\rm T}$, in order to test models of QCD energy loss more directly [20]. Jets are reconstructed using the anti-k_t algorithm with the jet size set to both R=0.2 and R=0.4, based on "towers" composed of calorimeter cells integrated over regions of size $\Delta\eta \times \Delta\phi = 0.1 \times 0.1$. The ambient background is removed at the cell level by excluding regions near jets and calculating the mean energy, as well as any azimuthal modulation, in strips of width $\Delta\eta = 0.1$. An iterative procedure is applied to remove any residual effect of the jets on the background subtraction. The final jets are corrected for the energy scale and resolution based on PYTHIA jets embedded into HIJING, with conservative systematic uncertainties assigned to account for the small differences between the fluctuations seen in data and simulation. Jets are restricted to $|\eta| < 2.8$, to stay within the main barrel and endcap regions of the calorimeter.

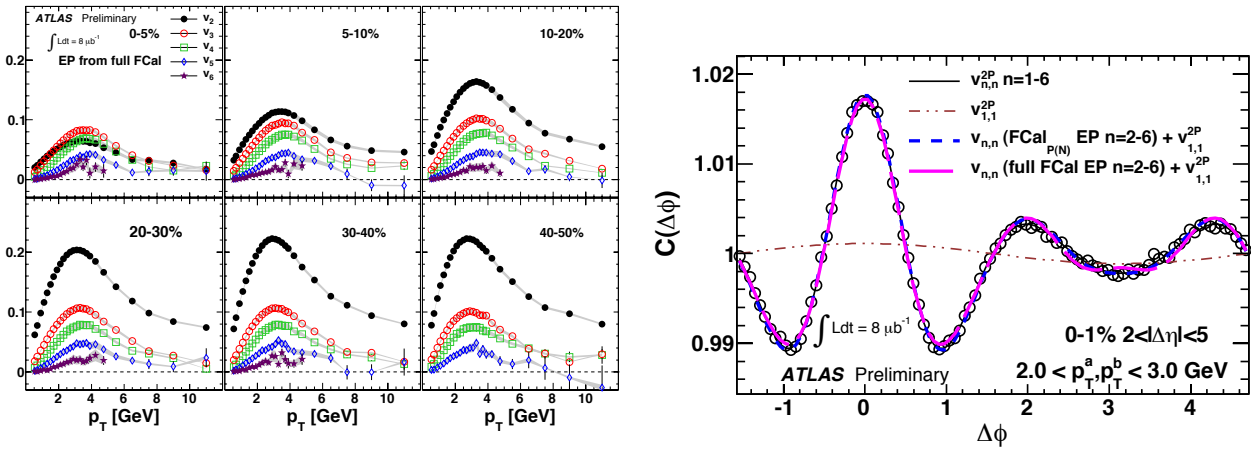

FIG. 6: (left) Higher order Fourier coefficients ($v_2 - v_6$) as a function of transverse momentum for six centrality bins, using the Event Plane (EP) method. It is observed that while v_2 varies strongly with centrality, $v_3 - v_6$ are nearly invariant. (right) Measured two-particle correlation function for $2 < p_{\rm T} < 3$ GeV and $\eta < 2.5$ in the 1% most central collisions (open circles). The reconstructed correlation function using the coefficients from the event plane measurement (and v_1 from the two-particle measurement) is also shown and agrees quite well with the directly measured correlation function, using both full FCal (solid line) and $\mathrm{FCal}_{\mathrm{P(N)}}$ (dashed line) methods.

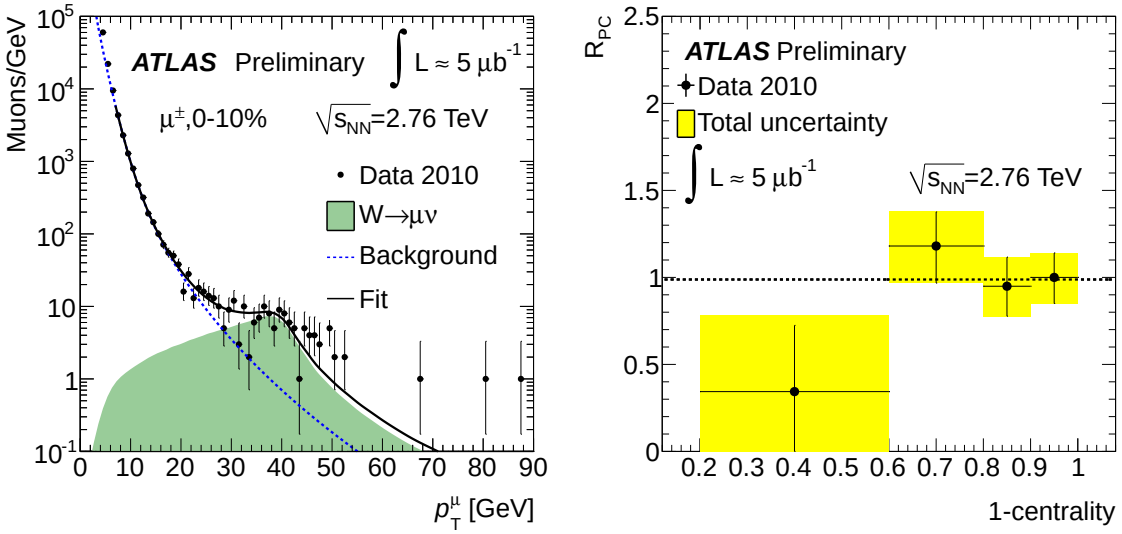

FIG. 7: (left) Single muon spectrum measured for the 0-10% most central events, with the templates for W bosons and heavy flavor (indicated as "Background") also shown to illustrate the yield extraction procedure. (right) R_{PC} for W bosons as a function of centrality, showing consistency with binary collision scaling. The dotted line is a fit to a constant.

The left panel of Figure 8 shows $R_{\rm CP}$ for R=0.4 jets, (defined similarly to $R_{\rm PC}$, but relative to the 60-80% centrality interval) as a function of centrality for jets in three fixed $E_{\rm T}$ bins ($E_{\rm T} = 50 - 75$ GeV, $75 - 100$ GeV and $100 - 125$ GeV). A smooth evolution of $R_{\rm CP}$ is observed going from the 50-60% central events on the right to the 0-10% central events on the left, where a suppression of roughly a factor of two is observed for all $E_{\rm T}$ bins and for both R=0.4 (left panel) as well as R=0.2 (shown the right panel). The invariance with R is suprising given the general tendency of radiative calculations to predict a modified fragmentation function for quenched jets, with substantial transverse broadening. However, direct measurements of the transverse and longitudinal fragmentation functions for tracks with $p_{\rm T} > 2$ GeV, shown in the left and right panels respectively of Fig. 9, confirm that no substantial modification of the fragmentation function can be observed when comparing peripheral and central events. In other words, the increased suppression of the jet rates is not

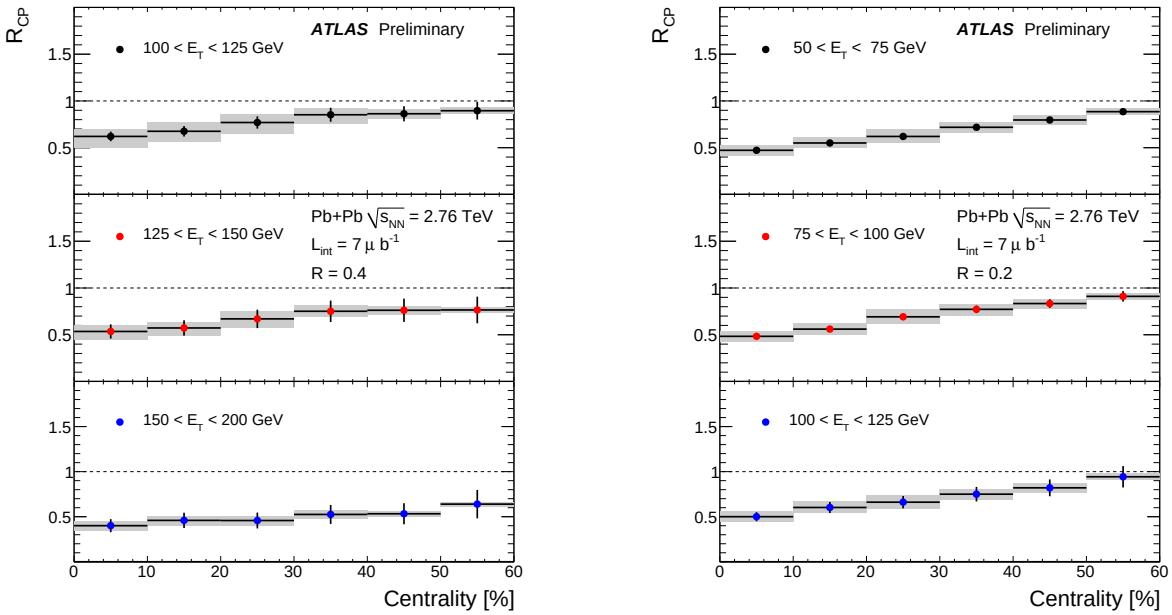

FIG. 8: (left) R_{CP} for R=0.4 jets, as a function of centrality, with 60-80% used as the peripheral sample. In this convention, the most central events are on the left and the most peripheral are on the right. (left) Similar as the other figure, but for $R = 0.2$.

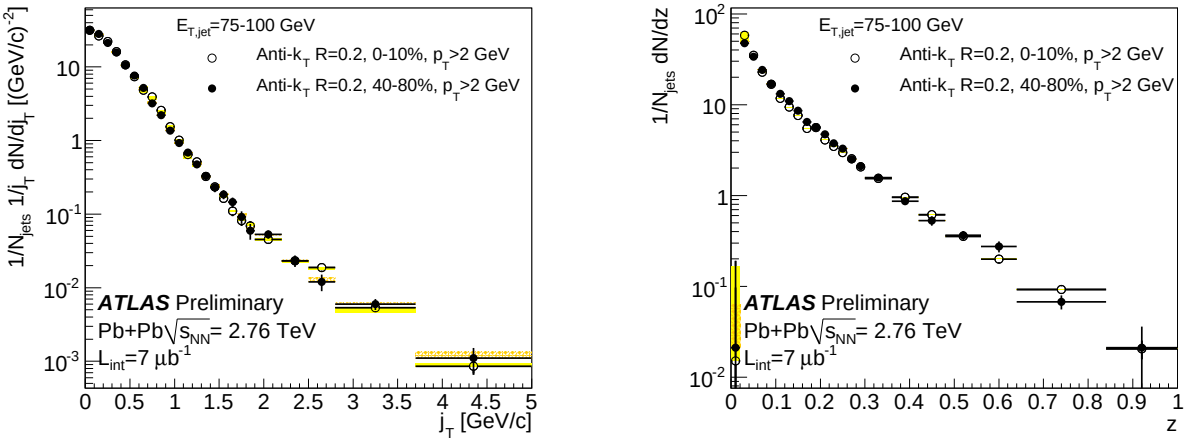

FIG. 9: (left) Transverse fragmentation function for R=0.2 anti-k_t jets, comparing central 0-10% events with peripheral 40-80%. (right) the similar comparison for the longitudinal fragmentation function.

accompanied by any evident modification of the jets themselves.

The original dijet asymmetry results provided the first direct evidence that jets lost energy through the hot, dense medium. The preliminary updated asymmetry results provide several major advances over the earlier ones. The full integrated luminosity ($L_{\rm int} = 7\ \mu{\rm b}^{-1}$ is now used, which increases the jet statistics by more than a factor of five. For the larger R=0.4 jets, the background subtraction now accounts for the effect of elliptic flow, using the measured event plane from the forward calorimeter and the $\cos(2\phi)$ modulation measured in the different calorimeter layers. Finally, a residual effect of the background subtraction on the reconstructed jet energy is removed using an iterative procedure that performs a second background subtraction excluding all reconstructed jets with $E_{\rm T} > 50$ GeV. This has an approximately 10% effect on jet energies.

The new results all use a leading jet with $E_{\rm T} > 100$ GeV and a subleading jet with $E_{\rm T} > 25$ GeV, with both jets within $|\eta| < 2.8$ and $\Delta\phi > \pi/2$. The cut in pseudorapidity is to exclude the ATLAS forward calorimeter,

in which the centrality and reaction plane measurements are made, and the cut in azimuth is to require the jets emerge in opposite hemispheres. The top panel of Fig. 10 shows the asymmetry distribution for reconstructed $R = 0.4$ jets, with the elliptic flow subtraction performed, in six centrality intervals. It is observed that the jets measured in the most peripheral bins resemble both fully simulated events with PYTHIA dijets embedded into HIJING background events, as well as proton-proton data at $\sqrt{s} = 7$ TeV. As the centrality is increased towards events with greater nuclear overlap, the distribution measured in lead-lead data becomes broader, and becomes essentially flat for the 0-10% most central events. It should be noticed that the slight "peak" structure seen in the original results [19] is no longer visible with higher statistics and better control over the background and jet energy. The middle panel of Fig. 10 shows the same results, but for R=0.2 jets. The identical trend is seen for these much smaller jets, which have a jet area a factor of four smaller relative to the R=0.4 jets and no flow subtraction. The fact that the asymmetry distribution similarly widens for the narrow jets, which are much less sensitive to residual background fluctuations, provides a counterargument to the one made in Ref. [21] that the asymmetry distribution could be explained by a poor understanding of the underlying event fluctuations. The bottom panel of the figure shows the distribution of $\Delta\phi$ between leading and subleading R=0.4 jets. In all centrality intervals, the emission remains primarily back-to-back. However, there is a low-lying but significant tail at $\Delta\phi < 3\pi/4$, which can presumaby be explained in part by the presence of fake jets.

To study this phenomenon further, charged particle yields have been measured out to $|\eta| = 2.5$ and $p_{\rm T} = 30$ GeV [22]. Tracks are reconstructed in the full inner detector (ID), with stringent requirements on the number of hits per track in order to suppress fake tracks. With these requirements, efficiencies are typically 70-80% while fake rates near $\eta = 0$ are less than a percent, although both efficiency and purity are degraded somewhat going to forward rapidity. While tracks are measured in ATLAS at transverse momenta well past 30 GeV, the measured track impact parameter errors (which are also used to reject fake tracks) are not the same in the data and in the present ATLAS simulations.

The top three panels of Fig. 11 show the corrected spectra out to 30 GeV, in three inclusive pseudorapidity intervals ($|\eta| < 0.35$, $|\eta| < 0.8$ and $|\eta| < 2.5$). The statistical errors are shown by the error bars (which are typically smaller than the graph markers) and total systematic uncertainties are shown by the light grey bands. Dividing the spectra by the yields measured in the 60-80% interval as well as the ratios of the number of binary collisions gives the charged-hadron R_{CP} values shown in the bottom three panels of Figure 11, for three centrality intervals relative to the 60-80% centrality interval. The trend for the 0-5% interval is similar to that seen in charged particle R_{AA} measured by ALICE [23]. There is a peak at 2-3 GeV, a minimum around 7 GeV and then a steady rise going out to high $p_{\rm T}$ which has not yet leveled-off even at $p_{\rm T} = 30$ GeV. The value of R_{CP} averaged over $p_{\rm T}$ from 20 to 30 GeV, shown in Fig. 12, is found to decrease smoothly from a value near unity for 50-60% to approximately 0.4 for the 0-10% most central collisions. This trend is both qualititatively and quantitatively similar to the one previously discussed for fully reconstructed jets.

IV. CONCLUSIONS

Results are presented from the ATLAS detector using over 9 $\mu{\rm b}^{-1}$ of lead-lead collisions from the 2010 LHC heavy ion run. The charged particle multiplicity increases by a factor of more than two relative to the top RHIC energy, with a centrality dependence very similar to that already measured at RHIC. Measurements of elliptic flow out to large transverse momentum also show similar results to what was measured at RHIC. Measurements of higher harmonics have also been made, which are able to explain structures in the two-particle correlation (e.g. the "ridge" and "cone" phenomena) previously attributed to jet-medium interactions. Single muons at high momentum are used to extract the yields of $W^{\pm}$ bosons as a function of centrality, which are found to be consistent with binary collision scaling. Conversely, jets are found to be suppressed in central events by a factor of two relative to peripheral events, with no significant dependence on the jet energy. Fragmentation functions are also found to be the same in central and peripheral events. Updated asymmetry results are presented for two different jet radii and improved background subtraction, confirming the first ATLAS results. Finally, charged hadrons have been measured out to 30 GeV, and the measured values of R_{CP} are found to have a centrality dependence (relative to peripheral events) similar to that found for jets.

Acknowledgments

The author would like to thank Derek Teaney and the DPF Heavy Ion session organizers for the invitation to speak at DPF 2011, and the ATLAS collaboration for their continued strong support of the ATLAS heavy ion physics program.

[1] ATLAS Collaboration, G. Aad et al., JINST **3**, S08003 (2008).
[2] ATLAS Collaboration, arXiv:1108.6027.
[3] ATLAS Collaboration, arXiv:1108.6018.
[4] ALICE Collaboration, K. Aamodt *et al.*, Phys. Rev. Lett. **106**, 032301 (2011).
[5] K. Aamodt et al., ALICE Collaboration, Phys. Rev. Lett. 105, 252302 (2010).
[6] A. Adare *et al.* PHENIX Collaboration, Phys. Rev. Lett. 105, 142301 (2010).
[7] J. Adams *et al.*, STAR Collaboration, Phys. Rev. **C72**, 014904 (2005).
[8] W. A. Horowitz, M. Gyulassy, arXiv:1107.2136, W.A. Horowitz, arXiv:1108.5876 (2011).
[9] W. A. Horowitz, private communication.
[10] W. A. Horowitz, M. Gyulassy, arXiv:1104.4958 (2011).
[11] B. Alver and G. Roland, Phys. Rev. **C81**, 054905 (2010) [Erratum-ibid. C **82**, 039903 (2010)].
[12] ATLAS Collaboration, ATLAS-CONF-2011-074 (`http://cdsweb.cern.ch/record/1352458`).
[13] J. Casalderrey-Solana, E. V. Shuryak, D. Teaney, J. Phys. Conf. Ser. **27**, 22-31 (2005).
[14] J. Adams *et al.*, Phys. Rev. Lett. **95**, 152301 (2005).
[15] A. Adare *et al.*, Phys. Rev. **C77**, 011901 (2008).
[16] B. I. Abelev *et al.*, Phys. Rev. **C80**, 064912 (2009).
[17] The ATLAS Collaboration, G. Aad *et al.*, Phys. Lett. **B697**, 294 (2011).
[18] ATLAS Collaboration, ATLAS-CONF-2011-078 (`http://cdsweb.cern.ch/record/1353227`).
[19] ATLAS Collaboration, G. Aad *et al.*, Phys. Rev. Lett. **105**, 252303 (2010).
[20] ATLAS Collaboration, ATLAS-CONF-2011-075 (`http://cdsweb.cern.ch/record/1353220`).
[21] M. Cacciari, G. P. Salam, G. Soyez, Eur. Phys. J. **C71**, 1692 (2011).
[22] ATLAS Collaboration, ATLAS-CONF-2011-079 (`http://cdsweb.cern.ch/record/1355702`).
[23] K. Aamodt *et al.*, Phys. Lett. **B696**. 30 (2011).

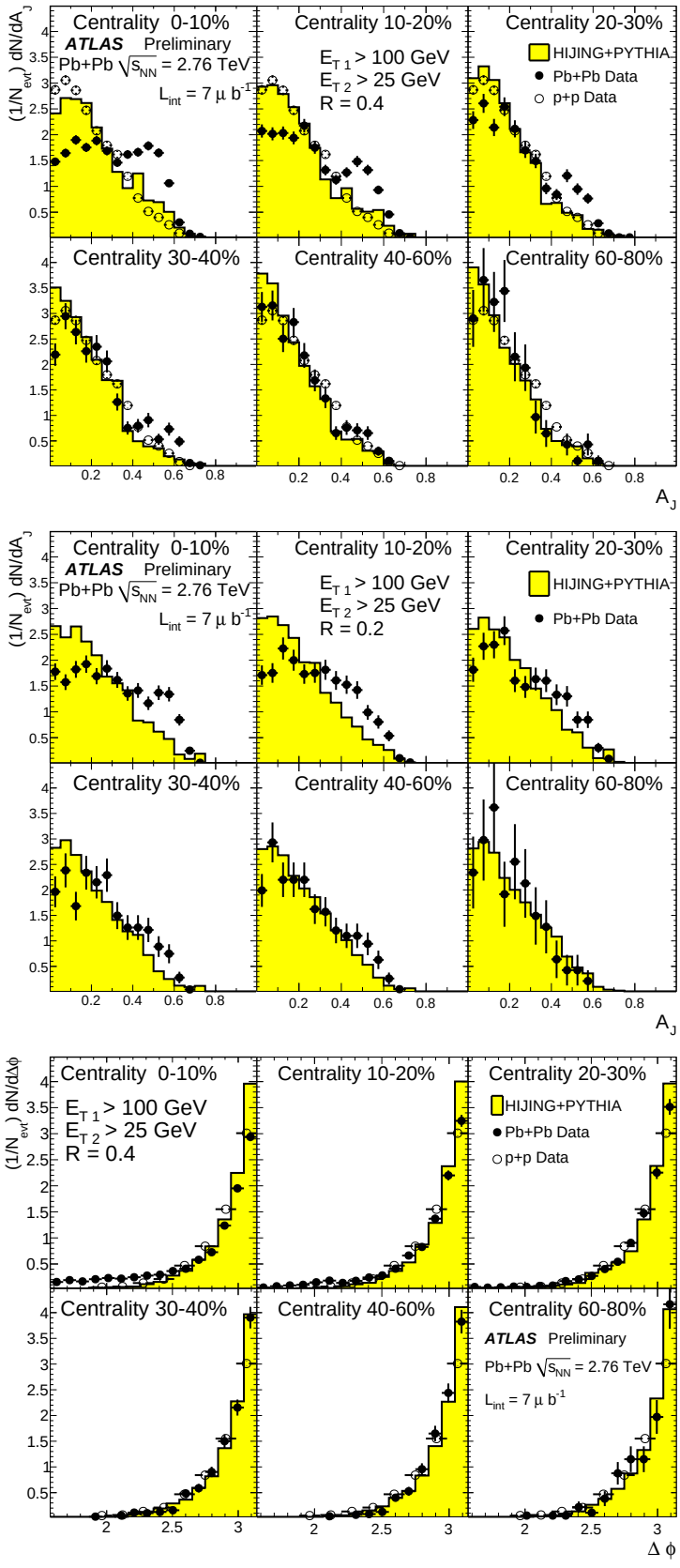

FIG. 10: (top) Asymmetry distribution as a function of centrality for $R = 0.4$ jets (middle) Asymmetry distribution as a function of centrality for $R = 0.2$ jets (bottom) $\Delta\phi$ distribution for $R = 0.4$ jets.

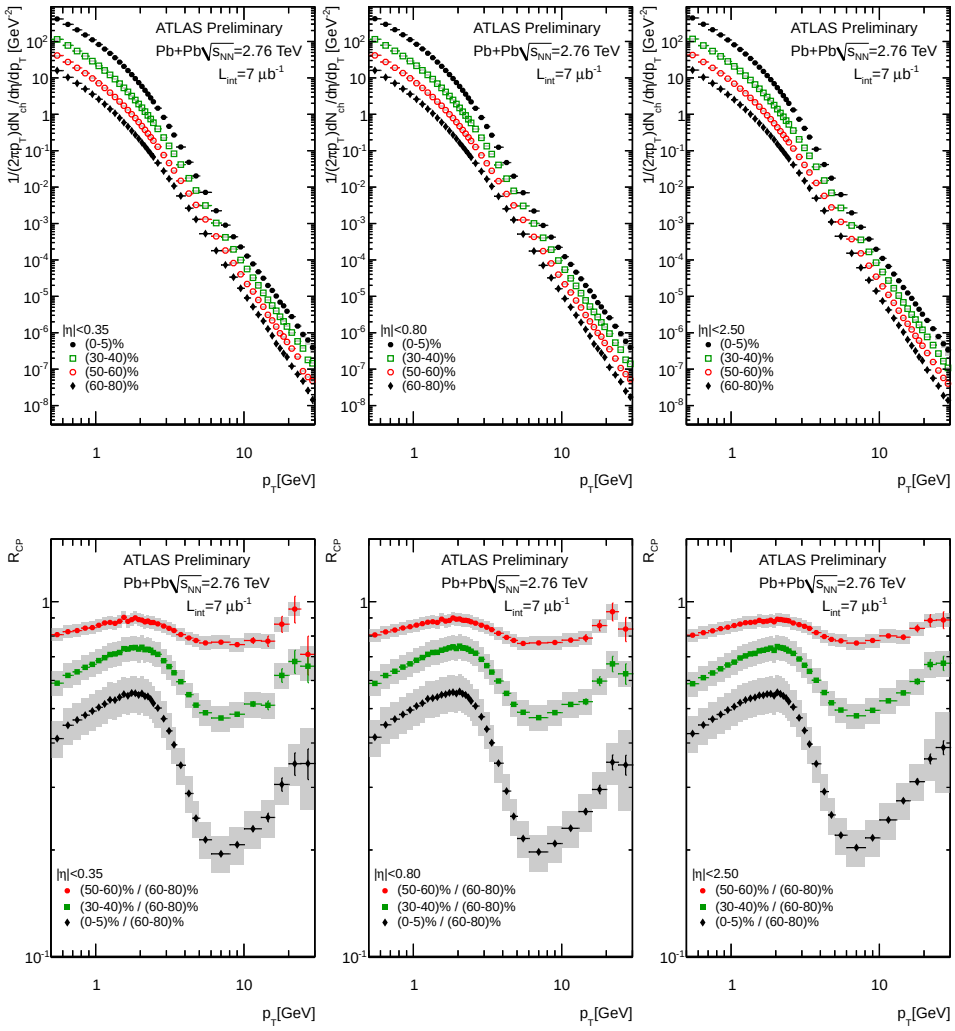

FIG. 11: (top) Invariant yields of charged particles for four centrality intervals and three inclusive pseudorapidity intervals. (bottom) Charged particle $R_{\rm CP}$ measured relative to the 60-80% bin, for all tracks measured within $|\eta| < 0.35$, $|\eta| < 0.8$ and $|\eta| < 2.5$.

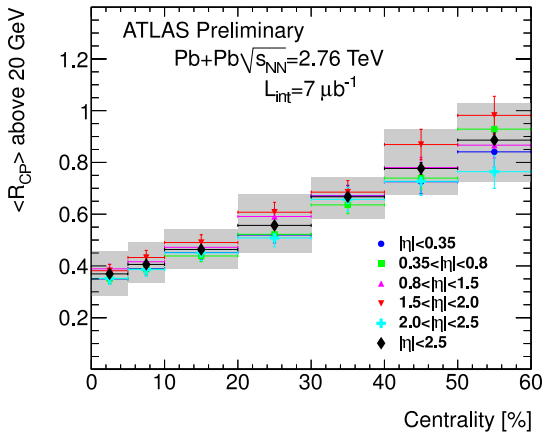

FIG. 12: $R_{\rm CP}$ for $p_T = 20 - 30$ GeV as a function of centrality, all relative to the 60-80% centrality interval.